Scientia Iranica, Vol. 15, No. 1, pp 57 64

SCIENTIA IRANICA

Turbulent Heat Transfer in a Channel with a Built-in Square Cylinder: The Effect of Reynolds Number

S.M. Hashemian[1], M. Rahnama[*] and M. Farhadi[2]

Turbulent heat transfer, in a three dimensional channel flow, in the presence of a square cylinder, was investigated numerically. The existence of a square cylinder in a channel, compared to a plain one, changes the heat transfer rate from the walls of the channel. A Large Eddy Simulation (LES) of a turbulent flow was performed to simulate flow behavior in a channel for Reynolds numbers in the range of 1000 to 15000. The results obtained for the Nusselt number distribution along the wall of the channel, at Re = 3000, followed those of experimental data with good accuracy. It was observed that the existence of a square cylinder makes the attached wall boundary layer separate, with a subsequent recirculation zone downstream of the cylinder. The Nusselt number distribution along the wall of the channel shows an increase, with a relative maximum, slightly downstream of the reattachment point. Heat transfer from the wall of the channel increases with increasing Reynolds number. A correlation was obtained for the variation of the mean total Nusselt number with the Reynolds number.

INTRODUCTION

Heat and mass transfer is affected by the structure of the flow near a surface. Separated flows, which appear in much engineering equipment, make remarkable quantitative and qualitative changes in various transport phenomena, such as heat and mass transfer. While such flows could be occurred around bluff bodies, even at low Reynolds numbers, there is no possibility of creating a separation in flow over a flat plate with a favorable pressure gradient. When a bluff body is placed near a flat plate, a vortical flow appears which, in turn, causes the attached flow over the flat plate to separate and a recirculation zone to appear over the plate. The existence of such recirculation zones creates an increase in heat transfer rate from the plate. The aim of the present paper is to investigate the effect that the Reynolds number has on the heat transfer from the wall of a channel in the presence of a turbulent promoter in the form of a square obstacle.

Various authors studied vortex shedding from a square cylinder [1-3]. The main objectives cover a wide range, from periodic forces exerted on the cylinder to the effect of confinement on flow and heat transfer. While the early studies of Davis and Moore [1] and Okajima [2] revealed the structure of a two-dimensional flow in detail, along with the effects of Reynolds number and geometrical parameters, such as the cylinder aspect ratio, there is still less recently published work about two-dimensional, small Reynolds number laminar flow across a square cylinder [4,5], which emphasizes the heat transfer from the cylinder. This shows that studies of heat transfer for a square cylinder have not been carried out to the same extent as those for fluid flow.

Actual flow around a square cylinder is three dimensional. It was reported by Breuer et al. [6] that a two-dimensional computation of flow over a square cylinder provides accurate results for Reynolds numbers less than around 200 and that there is uncertainty in computations obtained for Reynolds numbers greater than 300. Therefore, computation of flow and

1. *Department of Mechanical Engineering, Shahid Bahonar University of Kerman, Kerman, I.R. Iran.*
*. *Corresponding Author, Department of Mechanical Engineering, Shahid Bahonar University of Kerman, Kerman, I.R. Iran.*
2. *Department of Mechanical Engineering, Mazandaran University, Babol, I.R. Iran.*

heat transfer at higher Reynolds numbers should be done three-dimensionally, which is more complex and needs much more computational time. Another problem for higher Reynolds number flows in this geometry is that of selecting a proper type of turbulence model, especially a model which, also, predicts heat transfer accurately. Nakagawa et al. [7,8] studied turbulent structures in a channel flow with a rectangular cylinder and the unsteady turbulent near wake of the cylinder, experimentally, at a cylinder Reynolds number of 3000 and with a blockage ratio of 0.2. Four different aspect ratios were considered in their experiment: 0.5, 1, 2 and 3. They found out that the separated flow at the leading edge reattaches to the side walls of the cylinder for aspect ratios of 2 and 3, while they do not reattach and are entrained immediately behind the cylinder for aspect ratios of 0.5 and 1. They showed the contours of the phase-averaged vorticity and the streamline, as well as turbulent intensities and turbulent kinetic energy distribution in the near wake of the cylinder.

Kim et al. [9] studied turbulent flow past a square cylinder confined in a channel, numerically, using large eddy simulation. They used a dynamic subgrid-scale model with relatively fine grid points of $224 \times 144 \times 64$, with the aim of extensively verifying the experimental results of Nakagawa [8] and in order to identify the features of flows past a square cylinder, confined in a channel, in comparison with a conventional cylinder in an infinite domain. They showed that the vortices shed from the cylinder are significantly affected by the presence of the plate. Furthermore, they observed that periodic and alternating vortex-rollups exist in the vicinity of the plates, which are convected downstream, together with the corresponding Karaman vortex and which form a counter rotating vortex pair.

While most of the research work in the field of flows around rectangular cylinders has concentrated on fluid flow predictions in such geometries, a few authors tried to discover heat transfer prediction from the cylinder and/or channel walls. Turki et al. [10] studied unsteady flow and thermal fields around a heated square cylinder in a channel, numerically. The Reynolds number was selected as less than 200 and computations were performed for two blockage ratios of 1/4 and 1/8 and Richardson numbers from 0 to 0.1. The effect of natural convection in low Reynolds number flow situations was investigated. Some heat transfer correlations were also obtained for forced and mixed convection heat transfer from a plate. Most of the authors working in the field of heat transfer focused their attention on the heat transfer characteristics of a cylinder in a fluid flow at a low Reynolds number, while such geometry could be studied from another point of view, i.e., heat transfer from a channel floor, in channels subjected to a rectangular cylindrical obstacle. Nakagawa et al. [11], amongst others, pioneered the investigations into heat transfer in a channel flow, considering the effects of a rectangular cylinder placed in the middle of the channel. Experimental work was performed on heat transfer from the wall of a channel, in the presence of a rectangular cylinder at Re = 3000, based on cylinder height. This investigation was reported for cylinder aspect ratios of 0.5, 1, 2 and 3. It was observed that vortices shed periodically from the cylinder and reattach to the channel floor, which, in turn, induces a periodic fluctuation in heat flux at the floor and enhances heat transfer in the downstream region of the cylinder. It was also reported that the streamwise position of a maximum Nusselt number moves downstream with the decreasing width-to-height ratio of the cylinder.

The aim of the present study is to investigate, numerically, the effect of Reynolds number on convective heat transfer from the wall of a channel, in which a square cylinder is placed at its centerline. This geometry was investigated by a limited number of authors, but there is no investigation of such effects as Reynolds number on flow and heat transfer from the wall of the channel. The Reynolds number was selected between 1000 and 15000, which is based on cylinder height. For such a flow configuration, turbulent flow would appear around a cylinder. The turbulent model used in the present study was Large Eddy Simulation (LES), which requires a three-dimensional unsteady computation to get accurate results.

MATHEMATICAL FORMULATION AND COMPUTATIONAL DETAILS

Mathematical Model

Turbulent flow and heat transfer around bluff bodies at high Reynolds numbers can be modeled by LES, in which the larger, three-dimensional, unsteady, turbulent motions are directly represented, whereas the effects of small scales of motion are modeled through a filtering process. The equations for the evolution of the filtered velocity field are derived from Navier-Stokes equations. These equations are of a standard form, with the momentum equation containing the residual stress tensor. The application of the filtering operation to the continuity, Navier-Stokes and energy equations, gives the resolved equations, which, for incompressible flow, are as follows:

$$\frac{\partial \overline{u}_i}{\partial x_i} = 0, \tag{1}$$

$$\frac{\partial \overline{u}_i}{\partial t} + \frac{\partial}{\partial x_j}(\overline{u}_i \overline{u}_j) = \quad \frac{\partial \overline{p}}{\partial x_i} + \upsilon \nabla^2 \overline{u}_i \quad \frac{\partial \tau_{ij}}{\partial x_j}, \tag{2}$$

$$\frac{\partial \overline{T}}{\partial t} + \frac{\partial \overline{T} \overline{u}_j}{\partial x_j} = \frac{k}{\rho c} \nabla^2 \overline{T} \quad \frac{\partial q_j}{\partial x_j}, \tag{3}$$

where $\overline{p}$ is the pressure, $\overline{u}_1$, $\overline{u}_2$ and $\overline{u}_3$ are the filtered streamwise, cross-stream and spanwise components of velocity, respectively and $\overline{T}$ is the filtered temperature. These equations govern the dynamics of the large, energy-carrying scales of motion. The Reynolds number is defined as $U_0 h/\upsilon$, where U_0 and h are the uniform inlet velocity and cylinder height, respectively. The effect of small scales upon the resolved part of the turbulence appears in the subgrid scale (SGS) stress term, $\tau_{ij} = \overline{u_i u_j} \quad \overline{u}_i \overline{u}_j$, and the subgrid-scale heat flux term, $q_j = \overline{T u_j} \quad \overline{T}\,\overline{u_j}$, which should be modeled.

The main effect of the subgrid-scale stresses is dissipative, i.e., withdrawing energy from the part of the spectrum that can be resolved. One model for the subgrid-scale stress term, τ_{ij}, is based on its dependence on the filtered strain rate through an eddy-viscosity:

$$\tau_{ij} = \upsilon_t \left(\frac{\partial \overline{u}_i}{\partial x_j} + \frac{\partial \overline{u}_i}{\partial x_j} \right) + \frac{1}{3} \tau_{kk} \delta_{ij}, \tag{4.1}$$

$$q_j = \alpha_t \frac{\partial \overline{T}}{\partial x_j}. \tag{4.2}$$

In this study, the eddy viscosity, υ_t, is evaluated using the subgrid-scale (SGS) model of the Structure Function (SF) and Selective Structure Function (SSF) models. α_t is obtained from the turbulent Prandtl number as $\mathrm{Pr}_t = \upsilon_t \alpha_t$. Details of the SF and SSF models can be found in Farhadi and Rahnama [12] and Métais and Lesier [13].

Numerical Method

The governing equations presented in the preceding section were discretized using a finite volume method with a staggered grid. The convective terms were discretized using the Central Difference (CD) scheme. For LES computations, an important issue is to use, at least, second order accuracy for both time and spatial discretization of the equations. The convective and diffusive fluxes in the momentum and energy equations were treated explicitly in the present computations. A third order Runge-Kutta algorithm is used for the time integration, in conjunction with the classical correction method at each sub-step. The continuity Equation 1 and the pressure gradient term in the momentum Equation 2 are treated implicitly, while the convective and diffusive terms are treated explicitly. This method, which is called a semi-implicit fractional step method, provides an approach that does not use pressure in the predictor step as in a pressure corrector method (such as the well-known SIMPLE family of algorithms). The linear system of pressure is solved by an efficient conjugate gradient method with preconditioning. Further details on the numerical method are given in Suksangpanomrung [14].

Computational Domain and Boundary Condition

The computational domain consists of a square cylinder in the middle of a channel, which is extended in a spanwise direction (Figure 1) as one cylinder height. The length of the channel was selected as 20h, in order to reduce the effect of inlet and outlet boundary conditions on the computational flow field. The width of the channel was selected as 5h. These dimensions were selected, based on previously published works [15].

No-slip boundary conditions were used for the walls of the square cylinder; uniform flow is assumed as the inlet boundary condition and the outlet boundary condition is of a convective type, with U_c equal to 75% of the mean velocity as follows:

$$\frac{\partial u_1}{\partial t} + U_c \frac{\partial u_1}{\partial x_1} = 0. \tag{5}$$

It is well known that such a convective boundary condition is capable of predicting unsteady flow behavior, at the exit, with good accuracy. The spanwise boundary condition was selected as periodic. Thermal boundary conditions were selected as constant heat flux for one of the channel walls, while the other wall and cylinder surfaces were insulated. A uniform temperature and a convective temperature boundary condition (similar to Equation 5) were selected for the inlet and outlet, respectively. The minimum grid spacing used for both x and y directions is 0.02h, with a grid expansion ratio of 1.08. A uniform grid distribution was used in the spanwise direction, with a grid spacing of 0.1h. The number of grids used in the present computations was $283 \times 125 \times 11$. It should be mentioned that the number of grid points has an important effect on computed flow and temperature fields. For the present computations, it was observed that a higher number of grid points did not significantly change the main flow parameters, such as the recirculation length and the Nusselt number variation. The CFL (Courant-Friedrichs-Lewy) number is less than one for all computations with a maximum value of 0.95. The average time in the simulation is 150 h/U_{inlet}, where U_{inlet} is the uniform velocity at the inlet.

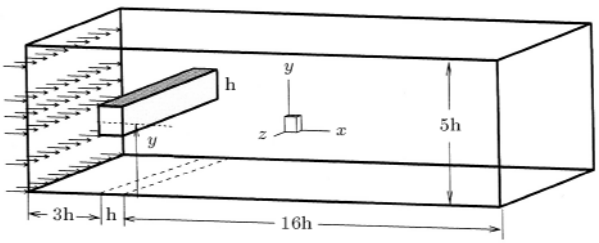

Figure 1. Flow configuration of channel with a built-in bluff body.

RESULTS

The geometry considered in this study consists of a three-dimensional square cylinder placed in a channel with a uniform velocity at the inlet (Figure 1). The blockage ratio is 20% and, at first, the Reynolds number, based on the uniform inlet velocity and cylinder height, was selected as 3000, in order to be able to compare the computational results with the experiments of Nakagawa et al. [8,11]. Secondly, the Reynolds number was changed from 1000 to 15000, in order to investigate its effect on flow and heat transfer from the floor of the channel (Figure 1). Finally, a correlation was obtained for the mean total Nusselt number of the channel wall.

Computational results obtained for the case of Re = 3000 are presented for the mean flow. Figure 2 shows the mean streamwise velocity component at the centerline for the symmetric plane, $z = 0$, downstream of the cylinder. It is observed that the results of present computations follow the experimental data of Nakagawa et al. [8]. To investigate the mean and fluctuating velocity components and Reynolds stresses at various Re numbers, Figure 3 was prepared, which shows various mean quantities at locations of $X = 1$, 2, 3.5 and 6. The first two sets of figures show streamwise and cross-stream velocities at these locations, along with the experiments of Nakagawa et al. [8] and very good correspondence is observed between these two data. The second two sets of the data are the variation of fluctuating velocity components, u' and v', along the channel in the above-mentioned locations. The mean streamwise fluctuating velocity component follows the experimental data with some small discrepancies, while the mean, cross-steam, fluctuating velocity component follows experimental data very well. The mean turbulent Reynolds stresses, $u'v'$, which are shown in the last set of Figure 3, follow the experimental data of Nakagawa et al. [8] with good accuracy. Such comparisons show that the present numerical scheme is capable of performing unsteady turbulent flow in the channel geometry with good accuracy.

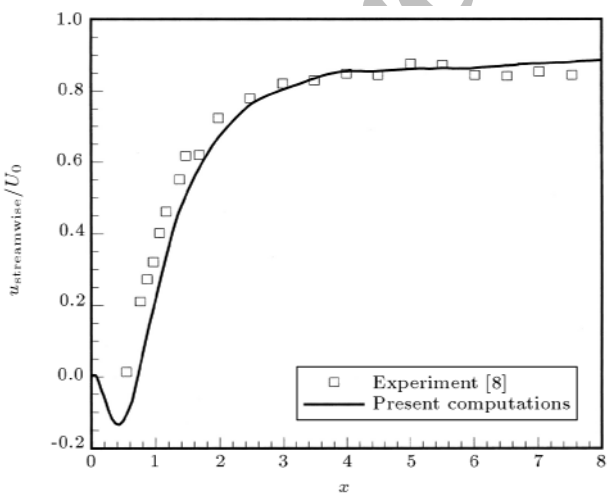

Figure 2. Variation of mean streamline velocity in plane of symmetry, $Z = 0$ versus x.

Regarding the main objective of the present paper, which is to investigate heat transfer from the channel floor, attention is directed toward the related parameters, such as temperature variation and Nusselt number distribution, along the bottom wall of the channel. The first computation was performed for the case of a uniform flow entering a straight channel with no obstacle, with an insulated top wall and a floor wall with a constant heat flux. Figure 4 shows the results of the present computations of Nusselt number for this case, along with the experimental data of Nakagawa et al. [11], which shows a good correspondence between these two sets of data. It should be mentioned that the definition of the Nusselt number was based on the constant heat flux of the plate and the height of the cylinder, $\mathrm{Nu} = q''h/k\Delta T$, in which ΔT is the temperature difference between the wall surface and inlet fluid.

Heat transfer from the floor of a channel with a square cylinder placed at the center of the channel at Re=3000 was the second geometry studied in the present work, the Nusselt number distribution for which is observed in Figure 5, along with the experimental data. The Nusselt number distribution shown in this figure is obtained by averaging the local Nusselt number in the z-direction. While there are slight differences in the upstream region of the obstacle, excellent agreement is observed between the present computations and experimental data for the region downstream of the cylinder. There is a point of maximum Nusselt number in the latter region, which occurs at $X = 9.58$. This point is slightly downstream of the reattachment point of the separated flow over the floor of the channel. Figure 6 shows the streamline plots of the mean flow downstream of the cylinder. It is observed that the wake downstream of the cylinder makes the attached flow over the wall of the channel separate and creates a recirculation region with a reattachment point downstream of the end point of the wake. The point of maximum Nusselt number occurs slightly downstream of this reattachment point; a phenomenon which is observed in all of the separated and reattached flows in other geometries, such as flow over a blunt flat plate [16].

While the present computations are able to predict a downstream Nusselt number accurately, discrepancies are observed at the region upstream of the cylinder, as mentioned earlier. Very fine grids could not be used, as the computational time increases drastically with the number of grid points and no high-speed

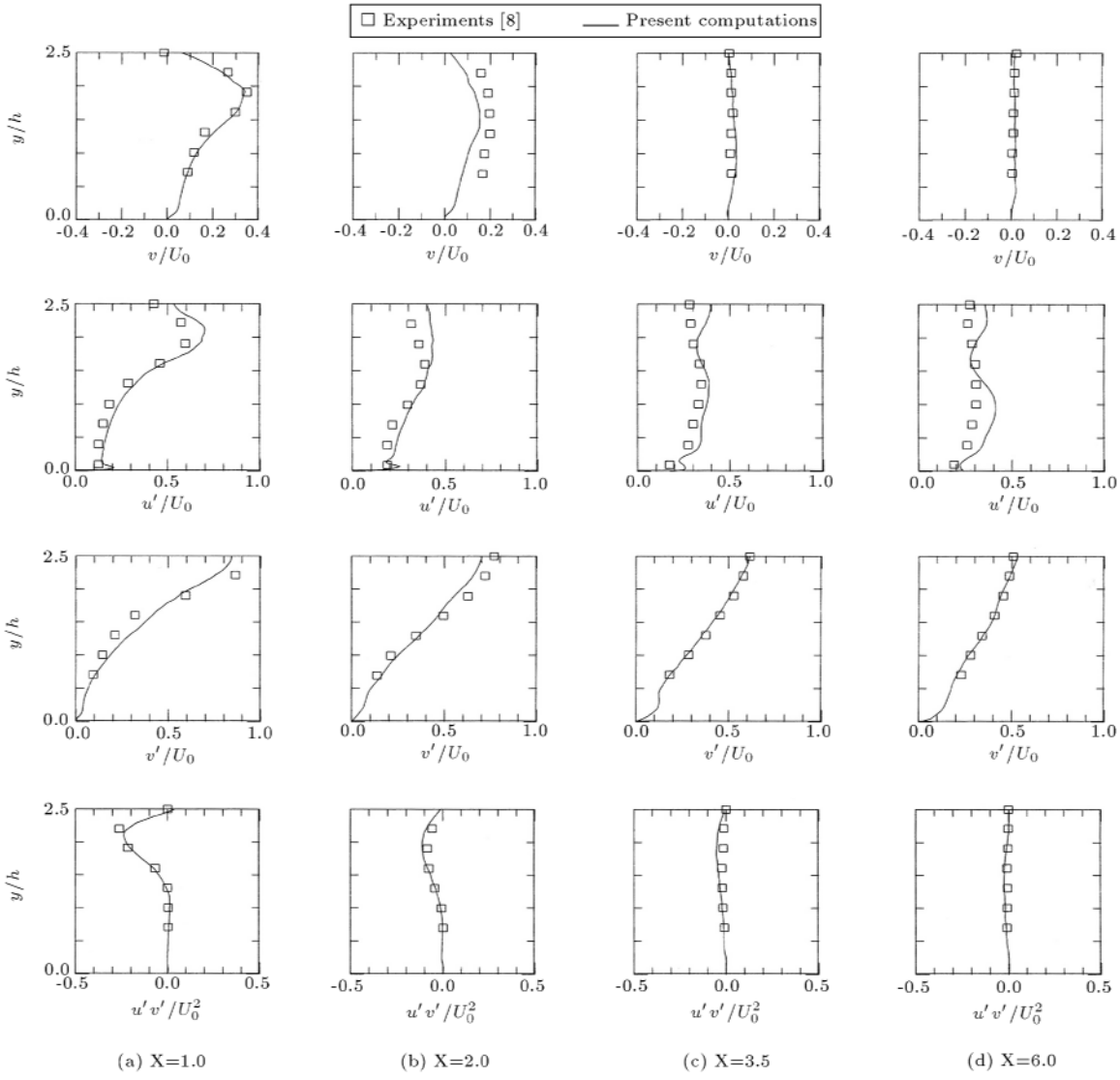

Figure 3. Distribution of velocity components and turbulent quantities in the symmetric plane of $Z = 0$.

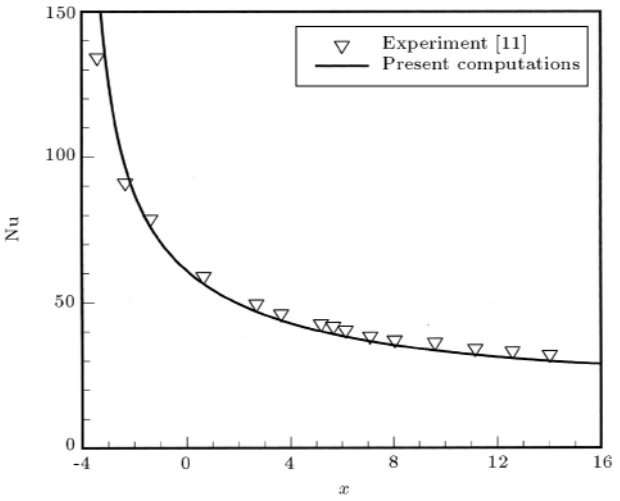

Figure 4. Nusselt number distribution along the floor of a channel without a square cylinder.

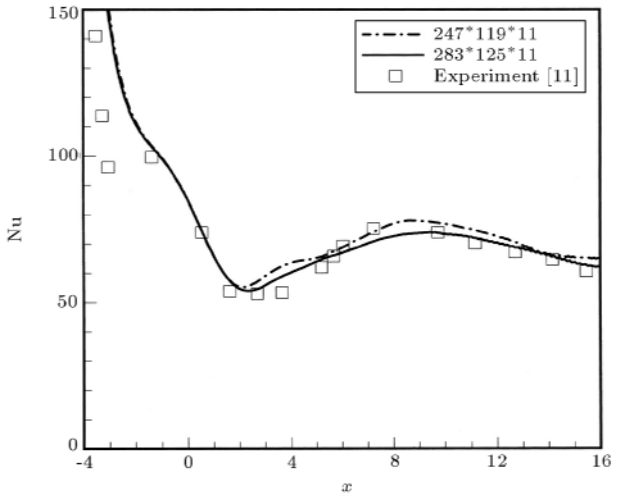

Figure 5. Nusselt number distribution along the floor of the channel with a built-in square cylinder at $\mathrm{Re} = 3000$.

computational facilities were available to the Authors, for undertaking such computations.

Figure 7 shows the Nusselt number distribution along the channel floor for Reynolds numbers of 1000, 3000, 5000, 10000 and 15000. As observed from this figure, the Nusselt number increases with an increasing Reynolds number and the position of maximum Nusselt number approaches the cylinder as the Reynolds number increases.

To more accurately investigate the effect of the recirculation region on Nusselt number variation along the floor of the channel, the instantaneous flow field, with the corresponding Nusselt number distribution, is shown in Figure 8 for Re = 3000. This figure shows the vorticity field at three different planes of $Z =$ 0.5, -0.1 and 0.3, along with the Nusselt number distribution for the floor at the same planes. It is clearly observed that

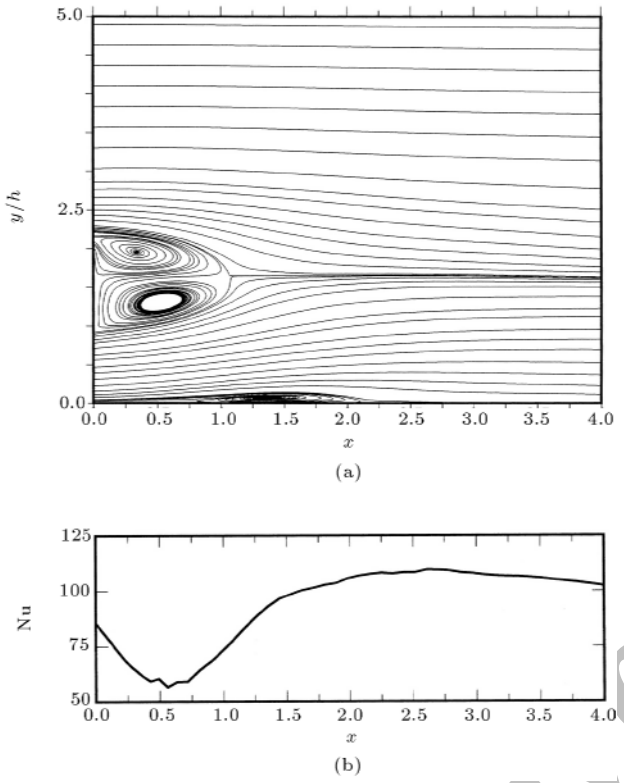

Figure 6. (a) Streamlines along the channel for the symmetric plane, $Z = 0$, and (b) Nusselt number distribution over the floor of the channel (square cylinder placed at $y_0/h = 1.5$).

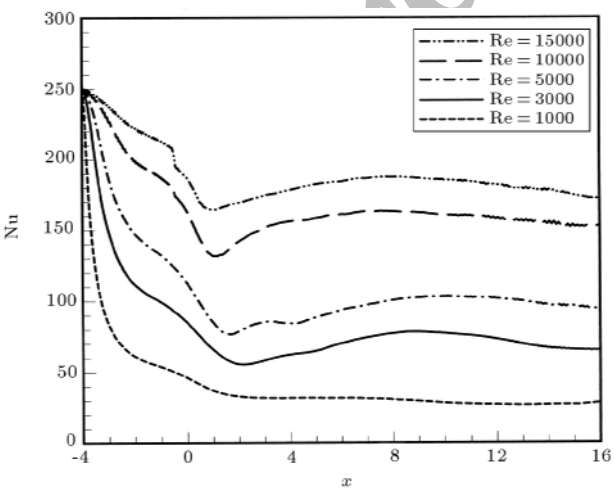

Figure 7. Nusselt number distribution along the floor of the channel for different Reynolds number.

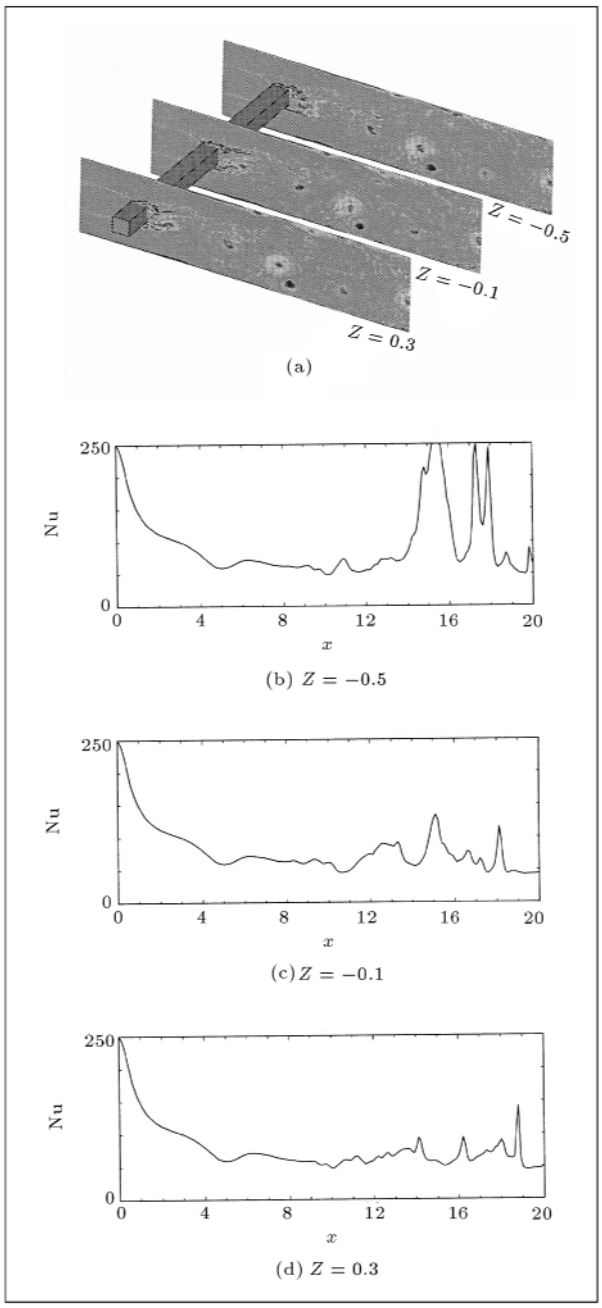

Figure 8. Instantaneous vorticity field at three sections of $Z =$ 0.5, -0.1 and 0.3, along with their respective Nusselt number distribution for Re = 3000.

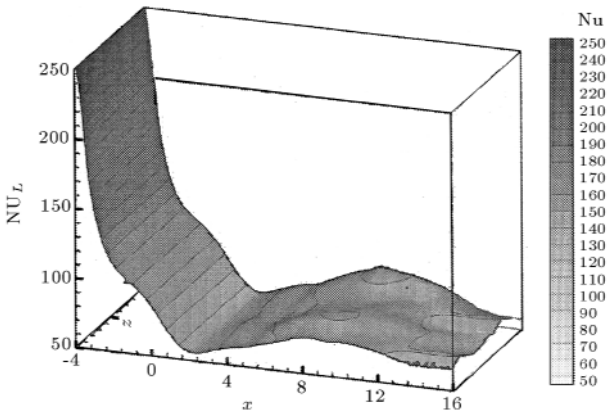

Figure 9. Nusselt number distribution over channel floor for the cylinder placed at $y_0/h = 1.5$.

the Karaman vortices generated, due to the existence of the cylinder in the channel, interact with the floor boundary layer and make a vortical flow appear near the channel floor, which makes a sharp variation in the Nusselt number.

To more accurately see the effect of the three-dimensionality of the flow on the mean Nusselt number distribution along the plate, the mean Nusselt number distribution was shown in Figure 9, as a function of both x and z. It is observed that the mean Nusselt number varies slightly in the z-direction for a constant x-value, especially in the downstream region of the cylinder. Therefore, it is not possible to study such two-dimensional flow configurations.

One of the parameters that show total heat transfer from the channel floor is the mean total Nusselt number for the entire floor of the channel. The parameter was defined as the ratio of the mean total Nusselt number to the mean total Nusselt number without the cylinder, $\mathrm{Nu}_t/\mathrm{Nu}_b$, and its variation is shown in Figure 10 for different Reynolds numbers. It is observed that, as the Re increases, the mean total Nusselt number also increases. A correlation for the mean total Nusselt number variation with the location of the cylinder was found, which is as follows:

$$\mathrm{Nu}_t/\mathrm{Nu}_b = 0.0754(\mathrm{Re}/\mathrm{Re}_b)^2 + 0.7995(\mathrm{Re}/\mathrm{Re}_b) + 0.2551. \quad (6)$$

It should be mentioned that this correlation was obtained for $1000 \leq \mathrm{Re} \leq 15000$.

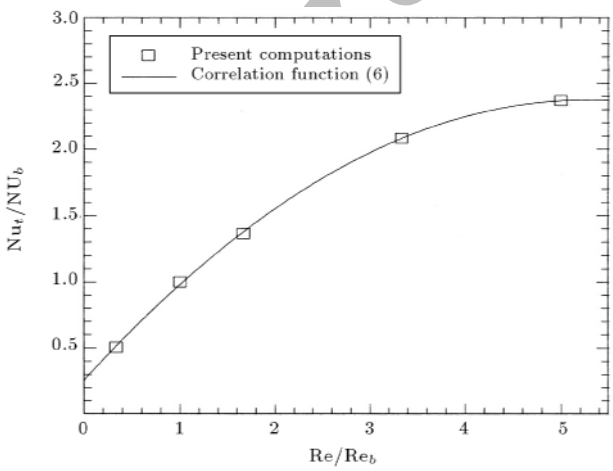

Figure 10. Mean total Nusselt number for different Reynolds numbers.

CONCLUSIONS

The effect of a square cylinder, placed in a turbulent channel flow, on the fluid field and heat transfer, was investigated, numerically, along with heat transfer from the floor of the channel. Regarding the main objective of the investigation, being the effect of the Reynolds number on heat transfer from the wall of the channel, the Reynolds number was selected as Re = 1000, 3000, 5000, 10000 and 15000. Using LES for the turbulence model, the following conclusions were obtained:

1. It was found that the presence of a cylinder disturbs the attached boundary layer on the floor and creates a recirculation zone near the wall, with subsequent reattachment, which, in turn, causes an increase in the Nusselt number. Its maximum occurs slightly downstream of the reattachment point;
2. The mean Nusselt number increases with an increasing Reynolds number. The point of the maximum Nusselt number approaches the cylinder as the Reynolds number increases;
3. A correlation was obtained for the variation of the mean rated Nusselt number with the Reynolds number (Equation 6).

NOMENCLATURE

c	specific heat of fluid
h	cylinder height
k	thermal conductivity
Nu_L	local Nusselt number, $\mathrm{Nu} = q''h/k\Delta T$
Nu	local Nusselt number averaged in z-direction
Nu_t	mean average Nusselt number for the entire floor of a channel with various Re
Nu_b	mean average Nusselt number for entire floor of a channel with $\mathrm{Re} = \mathrm{Re}_b$
$\mathrm{Nu}_{\max}$	maximum Nusselt numberover the channel floor
$\mathrm{Nu}_{\min}$	minimum Nusselt number over the channel floor
p	pressure

q''	subgrid scale heat flux
Re	Reynolds number based on the height of the cylinder, Uh/υ
Re_b	Reynolds number based on experimental data for comparison ($\mathrm{Re}_b = 3000$)
t	time
T	temperature
U_0	uniform inlet velocity
U_c	convective mean velocity
u_i	instantaneous velocity components
x_i	Cartesian coordinate, x_1, x_2, x_3
X	non-dimensional streamwise length, x/h
y_0	height of the cylinder above channel floor
Z	non-dimensional length, z/h

Greek Symbols

α_t	turbulent diffusivity
υ	kinematics viscosity
υ_t	turbulent viscosity
τ_{ij}	subgrid scale (SGS) stress tensor
ρ	density

REFERENCES

1. Davis, R.W. and Moore, E.F. "A numerical study of vortex shedding from rectangles", *J. Fluid Mech.*, **116**, pp 475-506 (1982).
2. Okajima, A. "Strouhal numbers of rectangular cylinders", *J. Fluid Mech.*, **123**, pp 379-398 (1982).
3. Davis, R.W., Moore, E.F. and Purtell, L.P. "A numerical-experimental study of confined flow around rectangular cylinders", *Phys. Fluids*, **27**(1), pp 46-59 (1984).
4. Dhiman, A, Chhabra, R.P. and Eswaran, V. "Flow and heat transfer across a confined square cylinder in steady flow regime: Effect of Peclet number", *Int. J. Heat Mass Transfer*, **48**(21-22), pp 4598-4614 (2005).
5. Sharma, A. and Eswaran, V. "Effect of channel confinement on the two-dimensional laminar flow and heat transfer across a square cylinder", *Num. Heat Transfer*, Part A, **47**, pp 79-107 (2005).
6. Breuer, M., Bernsdorf, J., Zeiser, T. and Durst, F. "Accurate computations of the laminar flow past square cylinder based on two different methods: Lattice-Boltzman and finite volume", *Int. J. Heat Fluid Flow*, **21**, pp 186-196 (2000).
7. Nakagawa, S., Senda, M., Yamagami, K., Nitta, K. and Kikkawa, S. "Turbulent structure in a channel flow with a rectangular cylinder", *Trans. Japan. Soc. Mech. Eng.*, **B64-602**, pp 1009-1017 (1998).
8. Nakagawa, S., Nitta, K. and Senda, M. "An experimental study on unsteady turbulent near wake of a rectangular cylinder in channel flow", *Exp. In Fluids*, **27**, pp 284-294 (1999).
9. Kim, D.-H., Yang, K.-S. and Senda, M. "Large eddy simulation of turbulent flow past a cylinder confined in a channel", *Comp. & Fluids*, **33**, pp 81-96 (2004).
10. Turki, S., Abbasi, H. and Ben Nasrallah, S. "Two-dimensional laminar fluid flow and heat transfer in a channel with a built-in heated square cylinder", *Int. J. Thermal Sciences*, **42**, pp 1105-1113 (2003).
11. Nakagawa, S., Senda, M., Kikkawa, S., Wakasugi, H. and Hiraide, A. "Heat transfer in channel flow around a rectangular cylinder", *Heat Transfer*, Japanese Research, **27**(1), pp 84-97 (1998).
12. Farhadi, M. and Rahnama, M. "Three-dimensional study of separated flow over a square cylinder by large eddy simulation", *Proc. IMECHE, Part G: Journal of Aerospace Engineering*, **219**, pp 1-9 (2005).
13. Métais, O. and Lesieur, M. "Spectral large eddy simulations of isotropic and stably-stratified turbulence", *J. of Fluid Mech.*, **239**, pp 157-194 (1992).
14. Suksangpanomrung, A. "Investigation of unsteady separated flow and heat transfer using direct and large-eddy simulations", PhD Thesis, Department of Mech. Eng., University of Victoria, Victoria, Canada (1999).
15. Rodi, W. "Comparison of LES and RANS calculations of the flow around bluff bodies", *J. Wind Engineering and Industrial Aerodynamics*, **69**, pp 55-75 (1997).
16. Djilali, N., Gartshore, I.S. and Salcudean, M. "Calculation of heat transfer in recirculating turbulent flow using various near-wall turbulence models", *Numerical Heat Transfer*, Part A, **16**, pp 189-212 (1989).